Proceedings of the 17th World Congress
The International Federation of Automatic Control
Seoul, Korea, July 6-11, 2008

Dynamic Modeling and Identification of a Complex-structured Parallel Robot

Jens Kroneis, Peter A. Müller and Steven Liu

Institute of Control Systems, University of Kaiserslautern, Germany
(e-mail: {kroneis,sliu}@eit.uni-kl.de, amueller@rhrk.uni-kl.de)

Abstract: In this paper a new strategy for dynamic modeling and parameter identification of complex parallel robots including parallel crank mechanisms is presented. Based on a model reduction strategy motivated by the structure of the parallel robot SpiderMill, kinematics and dynamics are derived in a compact form applying the modified Denavit Hartenberg method and the Newton-Euler approach. The obtained parameter-linear inverse dynamical description is reduced to a parameter-minimal form applying only an analytical reduction method. The rigid body parameters of the inverse dynamic model are identified by using optimized trajectories and linear estimators. Due to exclusively analytical reduction a physical interpretation of the parameters is possible. Through the whole modeling and verification process verified MSC.ADAMS models and Solid Edge models of the demonstrator SpiderMill are used.

Keywords: parallel robots; model reduction; parameter identification.

1. INTRODUCTION

In industrial applications the importance of parallel robots is more and more increasing. As a tradeoff to their many advantages over classical serial robots complex kinematic and dynamic descriptions are required to describe the behaviour of parallel robots. Their kinematics can be described by using standard and modified Denavit Hartenberg method (Kahlil and Kleinfinger [1986]) or the geometric approach (Tsai [1999]). But especially the derivation of the system dynamics with regard to the implementation of modern model-based control concepts is a challenging task. In general, two classes of strategies have to be distinguished for the derivation of system dynamics: variational or energy methods (e.g. Lagrangian dynamics) and geometry- or vector-based methods. The most common vector-based method is the Newton-Euler approach, where every rigid body of a mechanical system is cut free and dynamic equations are derived by solving balances of forces and torques. For serial robots, its recursive formulation is very effective, but in case of parallel robots the non-recursive formulation of the Newton-Euler approach is more appropriate (Tsai [1999]). A main advantage of the Newton-Euler method is the parameter-linear form of system dynamics which allows the use of linear estimators in the identification process. Therefore it is used here.
For reduction of modeling effort, the concept of equivalent point or lumped masses was applied previously to parallel robots with simple limb structure. In Stamper [1997] masses of connecting rods are halved and concentrated at adjacent joints, motivated by the assumption that their low weight has no significant influence on full system dynamics - which does not hold in our case. The Stewart platform in Lebret et al. [1993] is modeled using a strategy describing the moving platform and legs separately, not getting an explicit or compact model of the system dynamics. The approach can be applied for legs of low complexity and actuation in link direction only. In Pietsch [2003] also uncomplex links that allow an analytical reduction to point masses are considered. In this paper an entire tool-based reduction strategy, that regards manipulator's symmetry, for parallel robots with highly complex links is introduced. The reduction process is supported by using CAE tools.
To develop model-based control strategies parameters of the dynamic model have to be determined. In most cases parameters cannot be calculated exactly, even with very high effort. Especially for friction terms parameter identification strategies are required to improve model accuracy. In case of parallel robots parameter identification is a challenging task. Due to kinematic (and therefore dynamic) coupling between the links within the loops, a single link cannot be moved independently from others. Hence the dynamic parameters cannot be identified separately. Two special identification methods have been developed for parallel robots. In case of indirect identification (Grotjahn et al. [2004]) parameters of the rigid body model and friction terms are identified separately, identifying local system models as intermediate steps. The direct identification method (Abdellatif et al. [2004]) estimates rigid body and friction parameters in one step using optimized trajectories. In our case the latter is used to lower the identification effort. Friction is neglected because corresponding effects are not modeled in the used MSC.ADAMS model and hence cannot be identified. The identified model forms the basis for the development of modern model-based control concepts and planning of optimal trajectories.
In Sec. 2 the demonstrator SpiderMill is presented and a strategy for reduced order modeling is introduced. The implementation of the concept for the planar robot is performed in Sec. 3. The analytical model reduction to the parameter-minimal form and the direct paramter identification are explained in Sec. 4. Experimental results and

the physical interpretation of the identified parameters are presented in Sec. 5. Conclusions are drawn in Sec. 6.

2. REDUCED ORDER MODELING STRATEGY

2.1 Models of the SpiderMill

The planar parallel robot SpiderMill, considered in our paper, comprises a double redundant closed-chain structure, constructed with only revolute joints and standard aluminium profiles. Besides the physical demonstrator a rigid simulation model (Fig. 1) of the robot based on a multi-body systems (MBS) description is implemented in MSC.ADAMS. It supports the reduced order analytical modeling and is used for identification of model parameters and for verification of derived analytical models. Using the standard Newton-Euler approach to derive the inverse dynamic, all N_K bodys of a mechanical structure must be cut free and balances of forces and torques must be set up. For the more complex structure of the SpiderMill this results in a system of $6 \cdot 17 = 102$ equations. It is not efficient to solve them. To use the standard Newton-Euler method for the derivation of a parameter-linear description of the system dynamics, a new strategy is developed for the SpiderMill. It bases on two main ideas: one is the concept of equivalent lumped masses, the other is a stepwise physically motivated reduction method. The goal is a simplified model where dynamical properties are retained and particularities of parameter identification considered.

2.2 Concept of equivalent lumped masses

By using the principle of equivalent lumped masses (Pietsch [2003], Pisla and Kerle [2000]) rigid bodies are replaced by their discrete point masses without changing the dynamic behavior of the modified system. The result is a dynamic equivalent model. Two rigid mass systems are equivalent in terms of dynamics if

- their whole mass is equal
- they have the same center of mass
- the moments of inertia refered to the center of mass are equal.

This three conditions are described by

$$\begin{aligned} \sum m_j &= m \\ \sum m_j \cdot \mathbf{x}_j &= 0 \\ \sum m_j \cdot d_j^2 &= I \end{aligned} \tag{1}$$

where d_j is the distance between the position $\mathbf{x}_j$ of the surrogate mass m_j and the position $\mathbf{x}_i$ of center of gravity of the overall mass m. This principle is used to combine the components of the redundant parallel crank mechanisms of the SpiderMill and to reduce the coupling elements to single point masses.

2.3 Model reduction strategy

The introduced stepwise strategy will utilize the manipulator's symmetry and the principle of dynamically equivalent lumped masses for reduced order modeling.

Step 1 - Planar reduction: The complex spatial parallel manipulator SpiderMill is reduced to the virtual plane E_B,

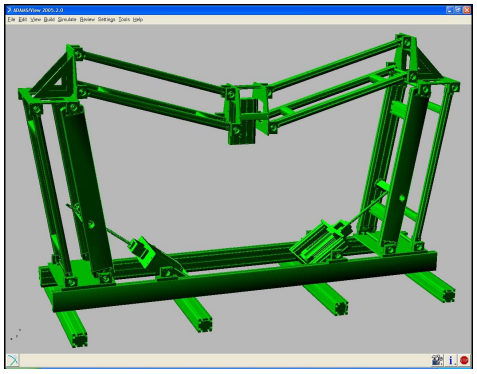

Fig. 1. MSC.ADAMS model of the SpiderMill

expressed by the coordinate frame ($\mathbf{e}_{x,EB}$, $\mathbf{e}_{y,EB}$), that is located symmetrically to the front and the back loop of the demonstrator. The axes of all rotational joints are perpendicular to E_B, so that end effector movements are reduced to this plane. By using these properties a reduced order model can be derived. Therefore elements that are symmetric to E_B and with common center of mass lying in E_B (verified using Solid Edge) are combined to one element, called group G_i (Fig. 2). It has been examined that effects of the unsymmetrically mounted end effector mass are negligible. Its center of mass is assumed to be in E_B. The reduced planar model is described by $3 \cdot 11 = 33$ equations.

Step 2 - Statically determinate model: Groups, whose parameters cannot be identified separately because they are always performing the same movements (e.g. G_7 and G_{11}), are combined in so-called substitution parts S_i (Fig. 3). They have the same kinematic properties as the involved groups and their dynamic properties are derived by using the principle of dynamically equivalent lumped masses. The positions of S_i are derived by determining the centers of mass of the involved groups using Solid Edge. Then the S_is are placed in a way that their longitudinal axes are parallel to that of the original groups and intersecting the new centers of mass (in Fig. 3 exemplarily shown for G_7 and G_{11}). However, the model is statically indeterminate. If S_1 and S_7 are resting, the other elements can still be moved. This is not possible for the real demonstrator. To get a kinematiclly correct model four vectors (Fig. 3) for each side of the manipulator are introduced ($\mathbf{r}_{G1,G2}$, $\mathbf{r}_{G2,G3}$, $\mathbf{r}_{G3,G4}$, $\mathbf{r}_{G4,G5}$ for left side). As S_2, S_4, S_6 do not rotate relative to the base coordinate frame ($\mathbf{e}_{x,B}$, $\mathbf{e}_{y,B}$), the dashed and the bold drawn vector loop are kinematically equivalent. Shifting S_1, S_3, S_5, S_7 along the vector loop leads to a M-structure. S_2, S_4, S_6

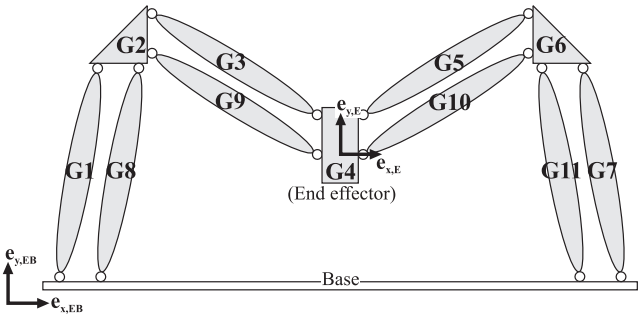

Fig. 2. Planar model with grouped components

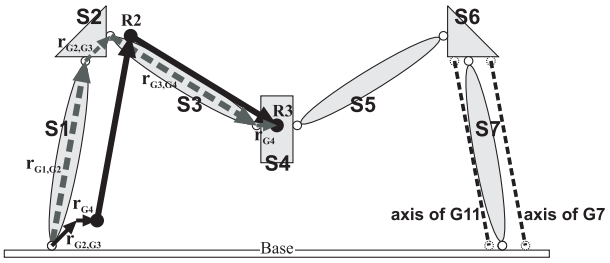

Fig. 3. Derivation of statically determined model

are dropped. Consequently the dynamic behavior of the M-structure is not equivalent to the real structure. To extend the M-structure the fact is used that S_2, S_4, S_6 cannot rotate relative to the base coordinate frame. Hence their dynamic behaviour is equivalent to point masses. To approximate the dynamic behavior of the real robot, the masses of S_2, S_4, S_6 are located at joints R_{2m}, R_{3m}, R_{4m} (filled out circles in Fig. 4). Although e.g. the distance between the base joints of G_1 and G_8 to the center of mass of G_2 (Fig. 2) is marginal longer than the length of S_1 (Fig. 3) this approximation leads to good results.

Step 3 - Full symmetrical modeling: For futher simplification the fact is used that the SpiderMill is a fully parallel robot with identical limbs. This implies that S_1 and S_7 are described by the same kinematic and dynamic parameters, as well as S_3 and S_5 so that just one symbol is used for e.g. the mass. Furthermore, using Solid Edge it has been verified for each substitution part S_i that one of its principal axes of inertia is identical with its longitudinal axes and another is perpendicular to E_B. Consequently, only the principal three moments of inertia are required for dynamic modeling. Due to the fact that all S_is are moving in E_B only one element of the tensor, which is identical for symmetrical parts (e.g. S_1 and S_7), is required. Because of the symmetrical construction of the robot the derivation of analytical equations is analogous for both sides, so that the modeling effort is reduced additionally.

Step 4 - Modeling of actuation: In the steps before the drive chains of the robot have not been regarded. Now ball screw systems acutating the axes are added (Fig. 4). The points of contact A_i are defined on the longitudinal axes of the substitution parts S_1 and S_7. At the real demonstrator the spindle bars are not mounted on the axes of symmetry of G_8 and G_{11}. Maintaining the distance d_A from the base joint to the contact point there is a small offset. It has been verified that the resulting error of the spindle orientations and therefore the effective directions of the spindle forces (forces in direction of ball screw systems) can be neglected. In the following joints R_1 and R_5 are considered as active.

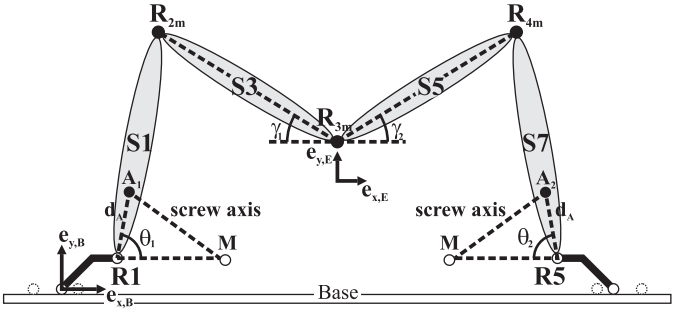

Fig. 4. SpiderMill: M-structure with actuation

Result: The complex spatial parallel manipulator SpiderMill is reduced to a simple planar M-structure with kinematic exact and dynamic well approximated behaviour. The application of the standard Newton-Euler approach to derive the inverse dynamic leads to a system of $3 \cdot 4 = 12$ equations instead of 102. An efficient analytical derivation of the inverse dynamics is now possible.

3. MODELING OF THE SPIDERMILL

The kinematics of the reduced model of the SpiderMill is derived by using the modified Denavit Hartenberg method. Therefore $\mathbf{q}_a = (\theta_1, \theta_2)$ are defined as active joint variables and two passive joint variables $\mathbf{q}_p = (\gamma_1, \gamma_2)$ are introduced. The verification of analytically derived kinematics with MBS simulation in MSC.ADAMS shows identical behavior within computational accuracy of the used programs.

For parameter identification using linear estimators an inverse dynamic model of the SpiderMill is required in a parameter-linear and parameter-minimal form. For this purpose the non-recursive Newton-Euler method is applied to the equivalent model (Fig. 4). The four substitution parts are cut free by taking the acting forces und moments as well as the required generalized velocities and accelerations into consideration (Sec. 2.3). As a result of the fact that the M-structure is limited to E_B three equations per substitution part arise. The resulting equation system is solved for the spindle forces to derive the inverse dynamic model.

Below the procedure is exemplarily shown for substitution part S_1 of the structure (Fig. 5). Its balances of forces and moments are given in (2) and (3). In general, certain forces can be avoided in the balances of moments by dexterous selection of centers of rotations.

$$
\begin{aligned}
&{}^0\mathbf{f}_0 + {}^0\mathbf{f}_{e1} - {}^0\mathbf{f}_1 + (0 \quad -m_1 g \quad 0)^T \\
&+ (0 \quad -m_2 g \quad 0)^T = m_1 {}^0\dot{\mathbf{v}}_{c1} + m_2 {}^0\dot{\mathbf{v}}_{c2} \qquad (2)
\end{aligned}
$$

$$
\begin{aligned}
&{}^0\mathbf{r}_{c1} \times (0 \quad -m_1 g \quad 0)^T + {}^0\mathbf{r}_1 \times (0 \quad -m_2 g \quad 0)^T \\
&+ {}^0\mathbf{r}_1 \times (-{}^0\mathbf{f}_1) + {}^0\mathbf{r}_{a1} \times {}^0\mathbf{f}_{e1} = m_1 {}^0\mathbf{r}_{c1} \times {}^0\dot{\mathbf{v}}_{c1} \\
&+ m_2 {}^0\mathbf{r}_1 \times {}^0\dot{\mathbf{v}}_{c2} + {}^0\mathbf{I}_1^{c1} \, {}^0\dot{\boldsymbol{\omega}}_1 + {}^0\boldsymbol{\omega}_1 \times ({}^0\mathbf{I}_1^{c1} \, {}^0\boldsymbol{\omega}_1) \qquad (3)
\end{aligned}
$$

Cutting free the substitution elements the whole mass of point mass m_2 is added to substitution part S_1 (in joint R_{2m}). This approach is motivated by practical considera-

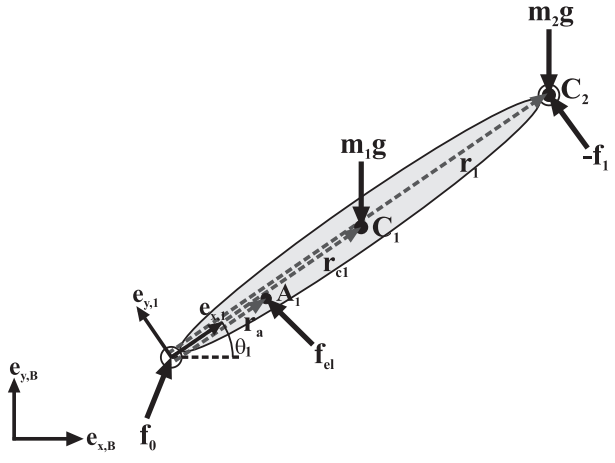

Fig. 5. Forces and moments on substitution part one

tions. At the real structure the motion of G_2 results form the rotation of G_1 and G_8 with reference to their base joints (Fig. 2). The distance between the center of mass of G_2 and the base joints of G_1 and G_8 is nearly equal to the length of substitution part S_1 of the reduced model. Consequently S_1 acts as lever arm and its actuation leads to an acceleration of m_2. The same approach is also used for modeling the right hand side of the SpiderMill. The mass m_4 of G_4 is partioned to S_3 and S_5.
By solving the balances of forces and moments for the spindle forces $\mathbf{f}_{e1}$ and $\mathbf{f}_{e10}$, the inverse dynamic model of the robot is obtained in parameter-linear form

$$\boldsymbol{\tau} = \mathbf{H}\left(\mathbf{q}, \dot{\mathbf{q}}, \ddot{\mathbf{q}}\right) \cdot \mathbf{p}_g \qquad \mathbf{q} = [\mathbf{q}_a, \mathbf{q}_p] \tag{4}$$

with $\boldsymbol{\tau}$ representing the vector of generalized forces, the vector $\mathbf{q}$ consisting of the active $\mathbf{q}_a$ and passive $\mathbf{q}_p$ joint variables, the matrix $\mathbf{H}\left(\mathbf{q}, \dot{\mathbf{q}}, \ddot{\mathbf{q}}\right)$ only containing known kinematic variables (e.g. lengths or angles) and $\mathbf{p}_g$ being the vector of dynamic parameters of the multi-body system. In case of the SpiderMill it contains eleven elements:

$$\begin{aligned} p_1 &= m_1 d_{c1} & p_4 &= m_3 & p_7 &= m_4 & p_{10} &= I_{c1,2} \\ p_2 &= m_1 d_{c1}^2 & p_5 &= m_3 d_{c3} & p_8 &= m_4 d_{c3} & p_{11} &= I_{c3,2}. \\ p_3 &= m_2 & p_6 &= m_3 d_{c3}^2 & p_9 &= m_4 d_{c3}^2 \end{aligned} \tag{5}$$

The derived inverse dynamic model is parameter-linear but not necessarily parameter-minimal. To obtain the parameter-minimal model of the robot, that is required for applying linear estimators, it is further examined using analytical methods.

4. PARAMETER IDENTIFICATION

4.1 Determination of basic parameters

Estimation of dynamic parameters of a rigid body system requires a full rank matrix $\mathbf{H}$. In this case the influence of one dynamic parameter on the generalized forces $\boldsymbol{\tau}$ is independent of the remaining ones and each of it is uniquely identifiable. Inverse dynamics is then called parameter-minimal. For determination of the minimal parameter set $\mathbf{p}_{min}$, parameters p_j not influencing the inverse dynamics - corresponding columns $\mathbf{h}_j$ of matrix $\mathbf{H}$ are zero - will be eliminated (Gautier and Khalil [1986, 1990], Grotjahn and Heimann [2000]).
Then the remaining parameters are regrouped to eliminate all linear dependencies between them. If the contribution of a parameter p_j to the inverse dynamics depends linearly on the contribution of other parameters $p_1^j \ \ldots \ p_{n_j}^j$, the corresponding colums of $\mathbf{H}$ are also linearly dependent

$$\mathbf{h}_j = \sum_{k=1}^{n_j} a_k^j \cdot \mathbf{h}_k^j \tag{6}$$

with constant linear factors a_k^j. Then parameter p_j and associated column $\mathbf{h}_j$ can be eliminated if the other parameters are replaced by

$$p_{k,neu}^j = p_k^j + a_k^j \cdot p_j \qquad k = 1 \ \ldots \ n_j. \tag{7}$$

The resulting inverse dynamics

$$\boldsymbol{\tau} = \mathbf{H}_R(\mathbf{q}, \dot{\mathbf{q}}, \ddot{\mathbf{q}}) \cdot \mathbf{p}_R \qquad \mathbf{q} = [\mathbf{q}_a, \mathbf{q}_p] \tag{8}$$

is examined for minimality in its parameters by using a sequence of samples $(\mathbf{q}, \dot{\mathbf{q}}, \ddot{\mathbf{q}})_{(i)}$, $i = 1 \ldots N$ and calculating the rank b of the matrix

$$\mathbf{W} = \begin{bmatrix} \mathbf{H}_R(\mathbf{q}, \dot{\mathbf{q}}, \ddot{\mathbf{q}})_{(1)} \\ \vdots \\ \mathbf{H}_R(\mathbf{q}, \dot{\mathbf{q}}, \ddot{\mathbf{q}})_{(N)} \end{bmatrix}. \tag{9}$$

If matrix $\mathbf{W}$ is full rank, the parameter-minimal form of the inverse dynamics is achieved:

$$\boldsymbol{\tau} = \mathbf{H}_{min}(\mathbf{q}, \dot{\mathbf{q}}, \ddot{\mathbf{q}}) \cdot \mathbf{p}_{min} \qquad \mathbf{q} = [\mathbf{q}_a, \mathbf{q}_p]. \tag{10}$$

The elements of $\mathbf{p}_{min}$ have an independent effect on $\boldsymbol{\tau}$. Otherwise, a numerical reduction strategy (Gautier [1990]) based on QR decomposition with pivoting has to be applied. But this generally leads to a loss of the physical interpretability of the parameters.

4.2 Direct identification

To estimate the dynamic parameters of the SpiderMill a trajectory optimally exciting the system (Abdellatif et al. [2004], Gautier and Khalil [1992], Presse and Gautier [1993], Swevers et al. [1997]) has to be generated. The required cost criterion and estimator will be presented below. The estimation is based on measurements of the generalized forces $\tilde{\boldsymbol{\tau}}_i$, the active joint variables $\tilde{\mathbf{q}}_{ai}$ and their derivatives $\dot{\tilde{\mathbf{q}}}_{ai}$ and $\ddot{\tilde{\mathbf{q}}}_{ai}$ at N equidistant time instants. A comparison of the measured and calculated generalized forces yields to an error $\mathbf{e}_i$.

$$\underbrace{\begin{bmatrix} \tilde{\boldsymbol{\tau}}_1 \\ \vdots \\ \tilde{\boldsymbol{\tau}}_N \end{bmatrix}}_{\tilde{\boldsymbol{\Gamma}}} - \underbrace{\begin{bmatrix} \mathbf{H}_{min}(\tilde{\boldsymbol{q}}_1, \dot{\tilde{\boldsymbol{q}}}_1, \ddot{\tilde{\boldsymbol{q}}}_1) \\ \vdots \\ \mathbf{H}_{min}(\tilde{\boldsymbol{q}}_N, \dot{\tilde{\boldsymbol{q}}}_N, \ddot{\tilde{\boldsymbol{q}}}_N) \end{bmatrix}}_{\boldsymbol{\Psi}} \cdot \mathbf{p}_{min} = \underbrace{\begin{bmatrix} \mathbf{e}_1 \\ \vdots \\ \mathbf{e}_N \end{bmatrix}}_{\boldsymbol{\eta}} \tag{11}$$

To minimize the quadratic error $\boldsymbol{\eta}^T \cdot \boldsymbol{\eta}$ the least-squares estimator

$$\mathbf{p}_{LS} = \left(\boldsymbol{\Psi}^T \cdot \boldsymbol{\Psi}\right)^{-1} \cdot \boldsymbol{\Psi}^T \cdot \tilde{\boldsymbol{\Gamma}} \tag{12}$$

with measurement vector $\tilde{\boldsymbol{\Gamma}}$ and information matrix $\boldsymbol{\Psi}$ is used. The analysis of the relative estimation error

$$\frac{\|\hat{\mathbf{p}}_{LS} - \mathbf{p}\|}{\|\mathbf{p}\|} \leq \underbrace{\|\boldsymbol{\Psi}\| \cdot \left\| \left(\boldsymbol{\Psi}^T \cdot \boldsymbol{\Psi}\right)^{-1} \cdot \boldsymbol{\Psi}^T \right\|}_{=\kappa(\boldsymbol{\Psi})} \cdot \frac{\|\boldsymbol{\eta}\|}{\|\boldsymbol{\Gamma}\|} \tag{13}$$

leads to a cost criterion to be met for optimally excitating the system to estimate the parameters. The relative estimation error decreases with the condition number $\kappa\left(\boldsymbol{\Psi}\right)$. The minimization of $\kappa\left(\boldsymbol{\Psi}\right)$, satisfying constraints for the active joints and their derivatives, leads to the following optimization problem:

$$\begin{aligned} \text{cost criterion:} \quad & \min_{\boldsymbol{\epsilon}} \kappa\left(\boldsymbol{\Psi}\right) \\ \text{trajectory:} \quad & \mathbf{q}_a = \mathbf{q}_a\left(t, \boldsymbol{\epsilon}\right) \\ \text{costraints:} \quad & \mathbf{q}_{a,min} \leq \mathbf{q}_a\left(t_k, \boldsymbol{\epsilon}\right) \leq \mathbf{q}_{a,max} \\ & \dot{\mathbf{q}}_{a,min} \leq \dot{\mathbf{q}}_a\left(t_k, \boldsymbol{\epsilon}\right) \leq \dot{\mathbf{q}}_{a,max} \\ & \ddot{\mathbf{q}}_{a,min} \leq \ddot{\mathbf{q}}_a\left(t_k, \boldsymbol{\epsilon}\right) \leq \ddot{\mathbf{q}}_{a,max} \\ & t_k \in [t_0, t_e] \qquad k = 1 \ldots N \end{aligned} \tag{14}$$

To solve this optimization problem a parametrizable function for the active joints $\mathbf{q}_{ai}\left(t, \boldsymbol{\epsilon}\right)$, whose parameters $\boldsymbol{\epsilon}$ are varied by a numerical optimizer, has to be selected. The result of the optimization are trajectories for the active joints that optimally excits the system to estimate the dynamic parameters. They are implemented in the

MBS model and $\tilde{\boldsymbol{\tau}}_i$, $\tilde{\mathbf{q}}_{ai}$, $\dot{\tilde{\mathbf{q}}}_{ai}$ and $\ddot{\tilde{\mathbf{q}}}_{ai}$ are determined and summarized in $\boldsymbol{\Psi}$ and $\tilde{\boldsymbol{\Gamma}}$. Using the least-squares estimator (12) the dynamic parameters of the inverse dynamic model are determined.

5. EXPERIMENTAL RESULTS

To verify the inverse dynamic model highly dynamic test trajectories for the active joints

$$\theta_i(t) = \theta_{i0} + \sum_{k=0}^{n_f} \left(\frac{\mu_k^i}{k\omega_f} \sin(k\omega_f t) - \frac{\nu_k^i}{k\omega_f} \cos(k\omega_f t) \right) \tag{15}$$

are defined. The trajectories are presented in Fig. 6. The verification of the inverse dynamic model requires the knowledge of the parameter vector $\mathbf{p}_{min}$. In a first step its unknown elements are taken from the MSC.ADAMS model (Table 1). By taken the test trajectories as motions for the active joints the calculated spindle forces of the analytical model solved in MATLAB are compared to the measured values of the MSC.ADAMS model (Fig. 6 e,f - dashed lines). Small relative errors occur. In Table 2 the average relative errors are presented. The errors of the reduced order model mainly result from the chosen locations for the point masses representing the upper coupling elements G_2, G_6 and the moving platform G_4 (Fig. 2). In the MBS model the lever arm from the base to the centers of mass of the triangulars and the lever arms from them to the center of mass of G_4 are longer than in the reduced model (Fig. 3). The marginal discrepance in modeling of the contact points A_i of the spindle forces additionally contributes to the error.

To further improve the analytical model, the dynamic parameters are no longer taken from the MBS model but rather identified using direct identification. The required parameter-minimal form of the inverse dynamics is achieved by using only analyctical reduction (derived in Sec. 4). This leads to the following minimal parameter set $\mathbf{p}_{min}$:

$$\begin{aligned}
p_{1,min} &= d_1 m_2 + d_1 m_3 + d_{c1} m_1 + \frac{d_1 d_{c3}}{2 d_3} m_4 \\
p_{2,min} &= d_1^2 m_2 + d_1^2 m_3 + d_{c1}^2 m_1 + \frac{d_1^2 d_{c3}}{2 d_3} m_4 + I_{c1,2} \\
p_{3,min} &= d_{c3} m_3 + \frac{d_{c3}}{2} m_4 \\
p_{4,min} &= m_4 - \frac{d_{c3}}{d_3} m_4 \\
p_{5,min} &= 2 d_{c3}^2 m_3 + d_{c3}^2 m_4 + 2 I_{c3,2}.
\end{aligned} \tag{16}$$

To estimate the parameters, trajectories optimally exciting the system are planed solving (14). As in Abdellatif et al. [2004] and Swevers et al. [1997] the trajectory is a finite Fourier series (15) with the following parameters:

$$\boldsymbol{\epsilon}^i = \begin{bmatrix} \theta_{i0} & \mu_1^i & \dots & \mu_7^i & \nu_1^i & \dots & \nu_7^i & \omega_f \end{bmatrix}^T \quad i = 1, 2. \tag{17}$$

The best condition $\kappa = 21.06$ is achieved for a Fourier series with length $n_f = 7$ and period $T_f = 7.29\,\mathrm{s}$. The trajectories are presented in Fig. 7. Using the trajectories as active joint motions the measurement vector $\tilde{\boldsymbol{\Gamma}}$ and the information matrix $\boldsymbol{\Psi}$ are dertermined and $\mathbf{p}_{min}$ is calculated using the least-squares estimator (12). To verify the improvements of the inverse dynamic model with the estimated parameter vector $\mathbf{p}_{min}$ the test trajectories (Fig. 6) and the identification trajectories (Fig. 7) for the active joints are used. For each trajectory the relative error of the inverse dynamic model with the estimated parameter vector $\mathbf{p}_{min}$ (Fig. 6/7 e,f - dashed lines) is significantly lower than the relative error of the inverse dynamic model with the parameters taken from MSC.ADAMS (Fig. 6/7 e,f - solid lines). A comparison of the average relative error of the test trajectories (Table 2) before and after the identification shows e.g. an improvement of the inverse dynamic model of 65.1 % for the spindle force $\mathbf{f}_{e1}$. Despite these

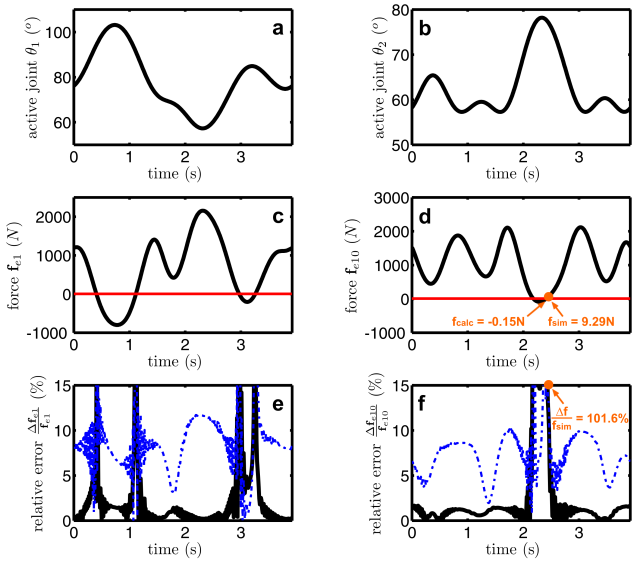

Fig. 6. Test trajectories for the left (a) and the right (b) active joint; forces of the left (c) and the right (d) spindle; relative error for MSC.ADAMS parameters (dashed line) and estimated parameters (solid line) of the left (e) and the right (f) spindle force

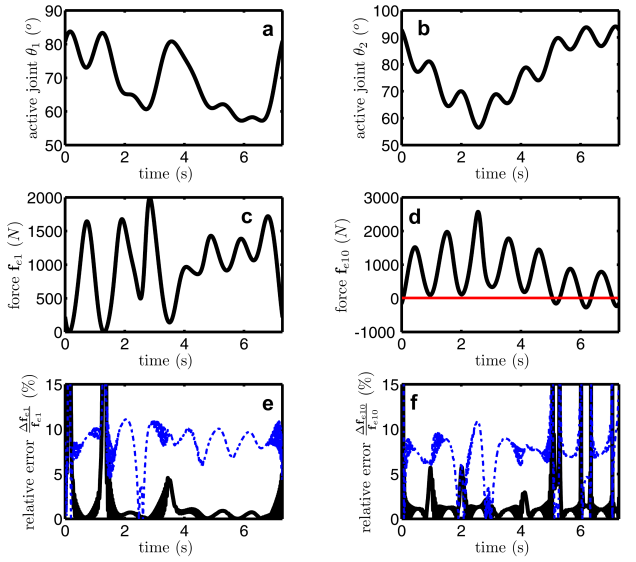

Fig. 7. Identification trajectories of the left (a) and the right (b) active joint; forces of the left (c) and the right (d) spindle; relative error for MSC.ADAMS parameters (dashed line) and estimated parameters (solid line) of the left (e) and right (f) spindle force

Table 1. MSC.ADAMS parameters and estimated parameters

MSC.Adams parameters	estimated parameters
$m_1 = 50.9597\,\mathrm{kg}$	
$m_2 = 7.9538\,\mathrm{kg}$	$m_2 = 15.9794\,\mathrm{kg}$
$m_3 = 14.5773\,\mathrm{kg}$	
$m_4 = 12.4560\,\mathrm{kg}$	$m_4 = 5.9203\,\mathrm{kg}$
$d_{c1} = 0.565\,\mathrm{m}$	
$d_{c3} = 0.515\,\mathrm{m}$	$d_{c3} = 0.833\,\mathrm{m}$
$I_{c12} = 6.3195\,\mathrm{kgm}$	$I_{c12} = 4.9733\,\mathrm{kgm}$
$I_{c32} = 1.6173\,\mathrm{kgm}$	$I_{c32} = 0.2162\,\mathrm{kgm}$

improvements the peaks in Fig. 6 e,f and Fig. 7 e,f have to be discussed. During the time span a peak arises the corresponding spindle force is close to zero. Then a small variation of the measured ($\mathbf{f}_{sim}$) and the calculated spindle force ($\mathbf{f}_{calc}$) results in a large relative error ($\boldsymbol{\Delta f}/\mathbf{f}_{sim}$), as exemplarily shown for one peak in Fig. 6.
Furthermore, the estimated parameters of $\mathbf{p}_{min}$ can be physically interpreted. To calculate the 8 dynamic parameters with (16), it must be assumed that 3 dynamic parameters are known. Because of the model reduction strategy presented in Sec. 2 it is suggestive to assume the masses m_2, m_4, the distance d_{c3} between R_{2m} and the center of mass of S_3 and the mass moments of inertia I_{c12}, I_{c32} as unknown. The results are presented in Table 1. The interpretation of the estimation is that an adjustment of I_{c12}, I_{c32} and a modification of point masses m_2, m_4 as well as a displacement of m_3 leads to an adapted reduced model with an improved behavior.
However the results in Table 1 show that it is not possible to estimate the real physical parameters of the SpiderMill because the inverse dynamic is calculated based on the reduced model. But through the parameter identification the inverse dynamic model is appreciably improved. Additionally the calculation of the 8 dynamic parameters allows the developement of model-based control strategies.

6. CONCLUSION

In this paper a new model reduction strategy for complex spatial parallel manipulators is presented. It uses manipulator's symmetry and the concept of dynamic equivalent lumped masses. Based on the reduced model the kinematics is derived by using the modified Denavit Hartenberg notation and the inverse dynamics is calculated by applying the Newton-Euler approach. Both are verified by using a MBS model. For this purpose the dynamic parameters are extracted from CAE tools. An improvement of the inverse dynamic model is achieved by applying direct parameter identification method. The required parameter-minimal form is achieved by using analytical reduction only. Consequently the physical parameters are calculated form the estimated parameter set so that a physical interpretation and application of model-based control strategies are possible. Because of its compact form the inverse dynamic model can be calculated with limited hardware resources. Hence the next steps are testing the identification strategy on the demonstrator also considering friction and the development of model-based control strategies.

Table 2. Average relative errors for the identification and the test trajectories with the calculated and the estimated vector $\mathbf{p}_{min}$

	identification	verification
calculated $\frac{\Delta \mathbf{f}_{e1}}{\mathbf{f}_{e1}}$	9.90%	10.20%
calculated $\frac{\Delta \mathbf{f}_{e10}}{\mathbf{f}_{e10}}$	9.08%	7.82%
estimated $\frac{\Delta \mathbf{f}_{e1}}{\mathbf{f}_{e1}}$	3.33%	3.56%
estimated $\frac{\Delta \mathbf{f}_{e10}}{\mathbf{f}_{e10}}$	3.30%	3.39%

REFERENCES

H. Abdellatif, F. Benimelli, B. Heimann, and M. Grotjahn. Direct identification of dynamic parameters for parallel manipulators. *Proc. of the Int. Conf. on Mechatronics and Robotics*, pages 999–1005, 2004.

M. Gautier. Numerical calculation of the base inertial parameters of robots. *IEEE Int. Conf. on Robotics and Automation*, pages 1020–1025, 1990.

M. Gautier and W. Khalil. A direct determination of minimum inertial parameters of robots. *IEEE Int. Conf. on Robotics and Automation*, pages 1682–1687, 1986.

M. Gautier and W. Khalil. Direct calculation of minimum set of inertial parameters of serial robots. *IEEE Trans. on Robotics and Automation*, 6(3):368–373, 1990.

M. Gautier and W. Khalil. Exciting trajectories for the identification of base inertial parameters of robots. *The International Journal of Robotics Research*, pages 362–375, 1992.

M. Grotjahn and B. Heimann. Symbolic calculation of robots' base reaction-force/torque equations with minimal parameter set. *13th CISM-IFToMM Symposium on the Theory and Practise of Robots and Manipulators (RoManSy)*, pages 59–65, 2000.

M. Grotjahn, B. Heimann, and H. Abdellatif. Identification of friction and rigid-body dynamics of parallel kinematic structures for model-based control. *Multibody System Dynamics*, 11(3):273–294, 2004.

W. Kahlil and J. F. Kleinfinger. A new geometric notation for open and closed-loop robots. *Proc. IEEE Int. Conf. on Robotics and Automation*, pages 1174–1179, 1986.

G. Lebret, K. Liu, and F. L. Lewis. Dynamic analysis and control of a stewart platform manipulator. *Journal of Robotic Systems*, 10(5):629–655, 1993.

I. T. Pietsch. *Adaptive Steuerung und Regelung ebener Parallelroboter*. PhD thesis, TU Braunschweig, 2003.

D. Pisla and H. Kerle. Development of dynamic models for parallel robots with equivalent lumped masses. *Int. Conf. on Methods and Models in Automation and Robotics*, pages 637–642, 2000.

C. Presse and M. Gautier. New criteria of exciting trajectories for robot identification. *IEEE Int. Conf. on Robotics and Automation*, pages 907–912, 1993.

R. E. Stamper. *A Three Degree of Freedom Parallel Manipulator with Only Translational Degrees of Freedom*. PhD thesis, University of Maryland, 1997.

J. Swevers, C. Ganseman, D. B. Tükel, and J. de Schutter. Optimal robot excitation and identification. *IEEE Trans. on Robotics and Automation*, pages 730–740, 1997.

L.-W. Tsai. *Robot Analysis - The Mechanics of Serial and Parallel Manipulators*. John Wiley & Sons, Inc., 1st edition, 1999.